Tropical Animal Health and Production (2023) 55:65
https://doi.org/10.1007/s11250-023-03487-6

REGULAR ARTICLES

Spatiotemporal and seasonality analysis of sheep and goat pox (SGP) disease outbreaks in Turkey between 2010 and 2019

Rumeysa Şener[1] · **Tarık Türk**[1]

Received: 28 April 2022 / Accepted: 23 January 2023 / Published online: 4 February 2023

Abstract

Sheep and goat pox (SGP) is a highly infectious disease with a high case fatality rate. It causes serious economic losses and decreases productivity in infected facilities and contact areas. As in many countries of the world, SGP outbreaks reported from Turkey to the World Organization for Animal Health (OIE) continue to threaten animal health. Therefore, studies that will guide the production of effective policies to prevent and control SGP are extremely important. This study aims at evaluating the spatiotemporal distribution of SGP outbreaks by geographical information system (GIS)–based analyses. In accordance with this purpose, spatiotemporal scan analyses were applied to reveal the spatiotemporal distribution pattern and transmission of SGP outbreaks reported in Turkey between 2010 and 2019. Space–time cluster analysis revealed 4 several clusters, indicating geographic areas at the highest risk. Spatiotemporal clusters were 6 to 11 times more likely to be exposed to SGP than the general distribution. The average spatiotemporal density of outbreaks in clusters was estimated as 0.20 ± 0.07 outbreaks per 1000 km^2 per month. Seasonal analysis and time series analysis showed similar findings. The seasonality of SGP was mainly defined in the winter (from December to February) when the seasonal adjusted factor (SAF) was at a peak of 504.6. In addition, February had the highest SAF with 7.1. Directional distribution analysis showed that the transmission of SGP was oriented between northeast (NE)–southwest (SW) and northwest (NW)–southeast (SE) and that distribution was changed every 2 years. These findings present a basis for the effective monitoring and prevention of SGP and provide valuable information to policymakers.

Keywords Sheep and goat pox · Spatial epidemiology · Spatial statistics · Time series analysis · Spatiotemporal clusters

Introduction

Sheep and goat pox (SGP) is a DNA virus belonging to the genus *Capripoxvirus* (CaPV) from the Chordopoxvirinae subfamily of the Poxoviaride family. SGP is a highly contagious viral infection that can affect sheep and goats with high morbidity and mortality rates. Clinically, SGP disease is characterized by fever, macules developing into papules, necrotic lesions in the skin, and nodular lesions in internal organs (Babiuk et al. 2009; AHA 2011; Kardjadj 2017). Although strains vary in their sensitivity to heat, poxvirus can generally survive for a long time by showing resistance to freezing and thawing, and resistance to drying and rot, under normal environmental conditions without susceptible animals (Rao and Bandyopadhyay 2000; Hurisa et al. 2018). The virus, which is inactivated by sunlight and heat, can survive up to 6 months in a cool and dark environment on a contaminated surface (Davies 1981; AHA 2011; Yune and Abdela 2017).

SGP is observed in Africa (except South Africa), Asia, and the Middle East, although not regularly in Greece and some Eastern European countries, north of the equator (Rao and Bandyopadhyay 2000; Kitching 2004; Radostits et al. 2006; Kardjadj 2017; OEI 2018). SGP is endemic in Nepal, China, Bangladesh, Ecuador, Iran, Turkey, Pakistan, Iraq, Afghanistan, the Indian subcontinent, and Africa (Mirzaie et al. 2015; Hurisa et al. 2018; OEI 2018). However, SGP is recognized as the most serious "pox" virus disease of ovine production animals in many parts of the world. SGP, which is not seen in Western and Central Europe and is considered exotic for the EU, is on the list of diseases that must be reported to the OIE (Yune and Abdela 2017; OEI 2018).

✉ Tarık Türk
tarikturk@gmail.com

[1] Department of Geomatics Engineering, Faculty of Engineering, Sivas Cumhuriyet University, 58140 Sivas, Türkiye

Generally, SGP can be infected by direct contact (as infectious animals) or indirect contact such as a contaminated object (Hurisa et al. 2018). The incubation period of sheeppox virus (SPPV) has been reported to be 4 to 8 days and goatpox virus (GTPV) to 4 to 15 days (House 1992). Restriction of animal movements is of great importance in the control of the disease, as the movement of infected animals causes the spread of SGP to new areas (Kitching and Taylor 1985; AHA 2011). It is also stated that SGP outbreak has the potential to cause serious economic losses in terms of reduced productivity in the affected herds in the livestock industries (EFSA 2014). At this point, the successful implementation of SGP outbreak control measures is frequently emphasized because it is of great importance in preventing the spread of the disease over different geographies (Carn 1993; Garner et al. 2000; Bhanuprakash et al. 2012).

Outbreaks of SGP from different geographical regions, from Turkey to OIE, were reported between 2010 and 2019. Routine control measures include the establishment of protection and surveillance zones, with a radius of 10 km, around the outbreaks as recommended by the Turkish Ministry of Agriculture and Forestry. In this direction, animals should be kept in a quarantine station for 21 days after final recovery or death and clinical/laboratory diagnosis. Sheep and goat flocks in disease-encountered areas should be vaccinated for a period of 2 years, followed by serological surveillance. Animal owners should be informed that the SGP virus persists for at least 3 months in the wool, hair, and scabs of infected animals and can survive in a cool, dark environment for up to 6 months. The outbreak zones should be disinfected and free of viruses (MAF 2018).

Spatial epidemiology, which has developed over the years and has been widely used, has focused on the use of spatial analysis and related statistical methodologies (Elliott et al. 2001; Kirby et al. 2017). Geographical information systems (GIS) have been utilized in several spatial epidemiology studies to reveal the relationships between the occurrences of diseases and their geographical environments (Cromley and McLafferty 2011). GIS have described the sources and geographical distributions of disease agents, identified the regions in time and space where animals may be exposed to pathological and environmental factors, and mapped and analyzed the spatial and temporal patterns in epidemic zones (Sui 2004; Caprarelli and Fletcher 2014). In addition, GIS provide critical tools for measuring spatial and temporal patterns that present information detailed on the occurrence of disease clusters or hotspots along with prevention and control of SGP (Waller and Gotway 2004; Şener 2021).

In many parts of the world, SGP is seen as a threat to animal health and economic development (EFSA 2014). The success of disease control measures depends on a clear examination of the epidemiology of SGP (Mirzaie et al. 2015; Kardjadj 2017; Hurisa et al. 2018). This study is focused on evaluating the spatial and temporal distribution of SGP outbreaks with GIS-based analysis models. The main objective of this study is to describe the temporal patterns and space–time clusters of SGP disease in sheep and goats. To better understand the infection dynamics, we are exposing the directional trend of SGP outbreaks and defining the direction of disease transmission. To better understand the temporal dynamics of SGP, we also analyze seasonal patterns in disease incidence. Thus, the findings of the study may provide guidance to policymakers on successful surveillance and control efforts, revealing the spatiotemporal epidemiological characteristics of SGP. At this point, these findings may inform control strategies in other regions where SGP is endemic and contribute to Turkey's attainment of SGP-free status.

Materials and method

Study area

This study was carried out within the borders of Turkey lying between 36–42° north latitude and 26–45° east longitude. The country, with an area of 783,562 km^2, stretches along the Anatolian peninsula in southwest of Asia. The country, partly located in the Balkan region of Southeastern Europe, stands out with its feature of being an intercontinental country in Eurasia, which is the connector of Europe and Asia (Fig. 1A). Turkey consists of seven geographical regions, namely the Mediterranean, Eastern Anatolia, Aegean, Southeastern Anatolia, Central Anatolia, Black Sea, and Marmara regions. It is located between the temperate zone and the subtropical climate zone, with climatic characteristics varying according to the regions (Dogru et al. 2017). Turkey consists of 81 provinces and 973 districts (Fig. 1B).

Data source and collection

Animal health data

SGP outbreak data reported in Turkey between 2010 and 2019 were obtained from the Republic of Turkey Ministry of Agriculture and Forestry. They include outbreak notifications of sheep and goats, suspects/affected/deaths (dead, killed, destroyed), disease confirmation and dispatch dates, and outbreak notification locations between 2010 and 2019. SGP has been reported at a total of 371 district locations. A total of 934 outbreaks were reported and 20,309 cases were recorded.

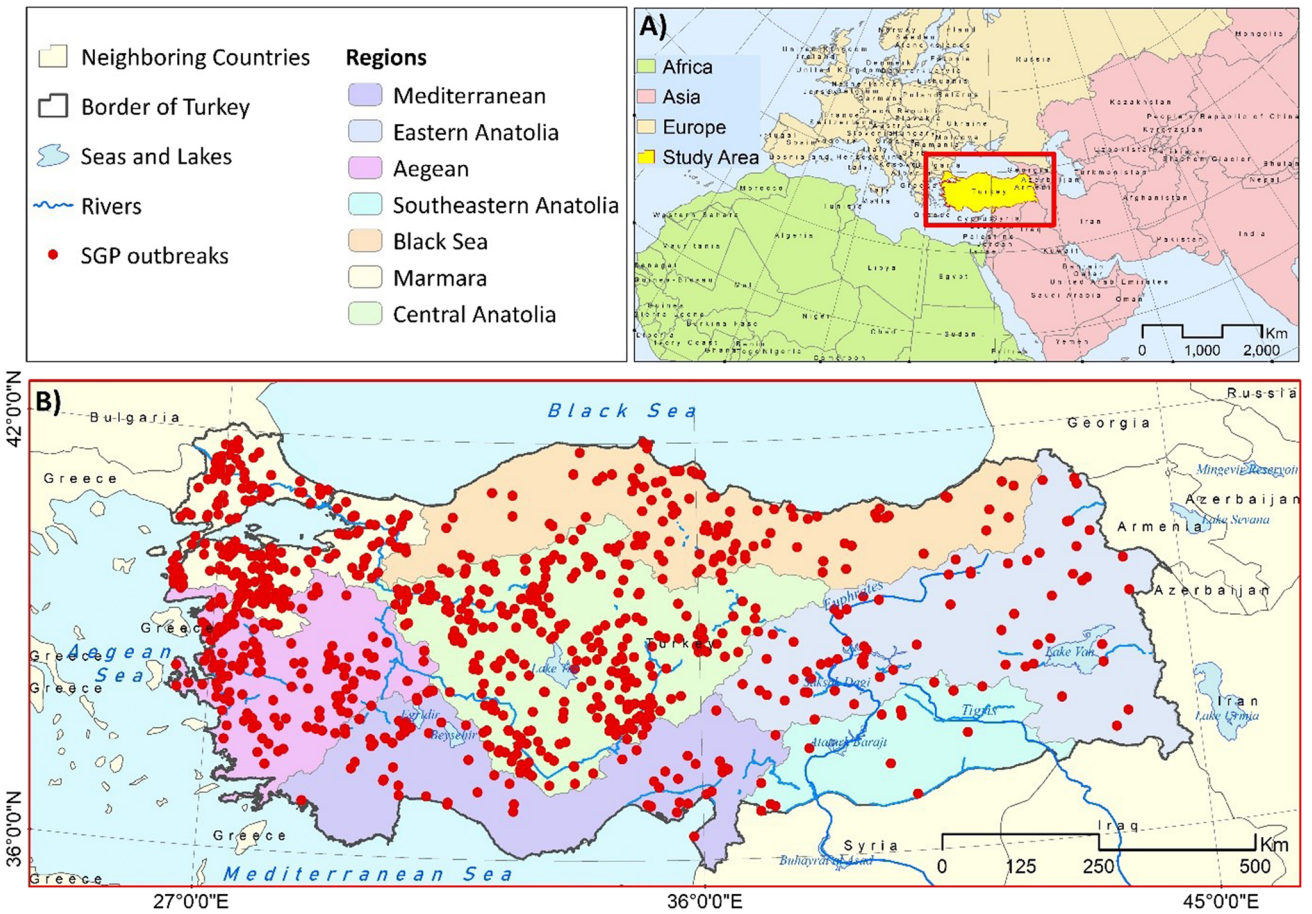

Fig. 1 **A**) The study area. **B**) SGP outbreak locations reported in Turkey between 2010 and 2019

Animal population data

Sheep and goat populations were obtained from Turkish Statistical Institute (TurkStat 2020) based on specific districts where outbreaks were reported between 2010 and 2019. The data included the sheep and goat population of the district where the outbreak is seen each year. Within the scope of this study, geographical data were used together with animal health and population data. The steps followed in the study are given in Fig. 2.

Seasonal decomposition analysis

The time series included 120 months in total between January 2010 and December 2019 and was examined by the seasonal decomposition. The seasonal decomposition procedure based on loess (STL) was applied in order to assess the trend and seasonality of SGP (Mao et al. 2020). This statistical technique was based on the decomposition of a time series dataset into three components: trend, seasonal, and remainder or residual on a yearly basis (Lee et al. 2017). Using the additive model, the decomposition procedures on the time series of SGP were compiled by summing three components into:

$$Z_t = T_t + S_t + R_t \quad (1)$$

where Z_t represents the monthly SGP incidence rates. T_t represents a trend component that reflects the long-term progression and non-periodic fluctuations of the series. S_t symbolizes the seasonal variation, reflecting the seasonality that occurs during a fixed and known period. R_t indicates the remaining component, which describes random, erratic effects after other components are removed.

A seasonal pattern is existed when a time series is influenced by seasonal factors (Khaliq et al. 2015). The peak of seasonal variation was determined by the seasonal adjusted factor (SAF). The stationarity of the data was checked by autocorrelation function (ACF) and partial autocorrelation function (PACF). The Ljung–Box test was employed to describe the structure and seasonality (stationary or non-stationary). In addition, a seasonal scan statistic was used which ignores the year of the observation and retains only the day and month to detect the seasonal cluster of SGP (Kulldorff 2018).

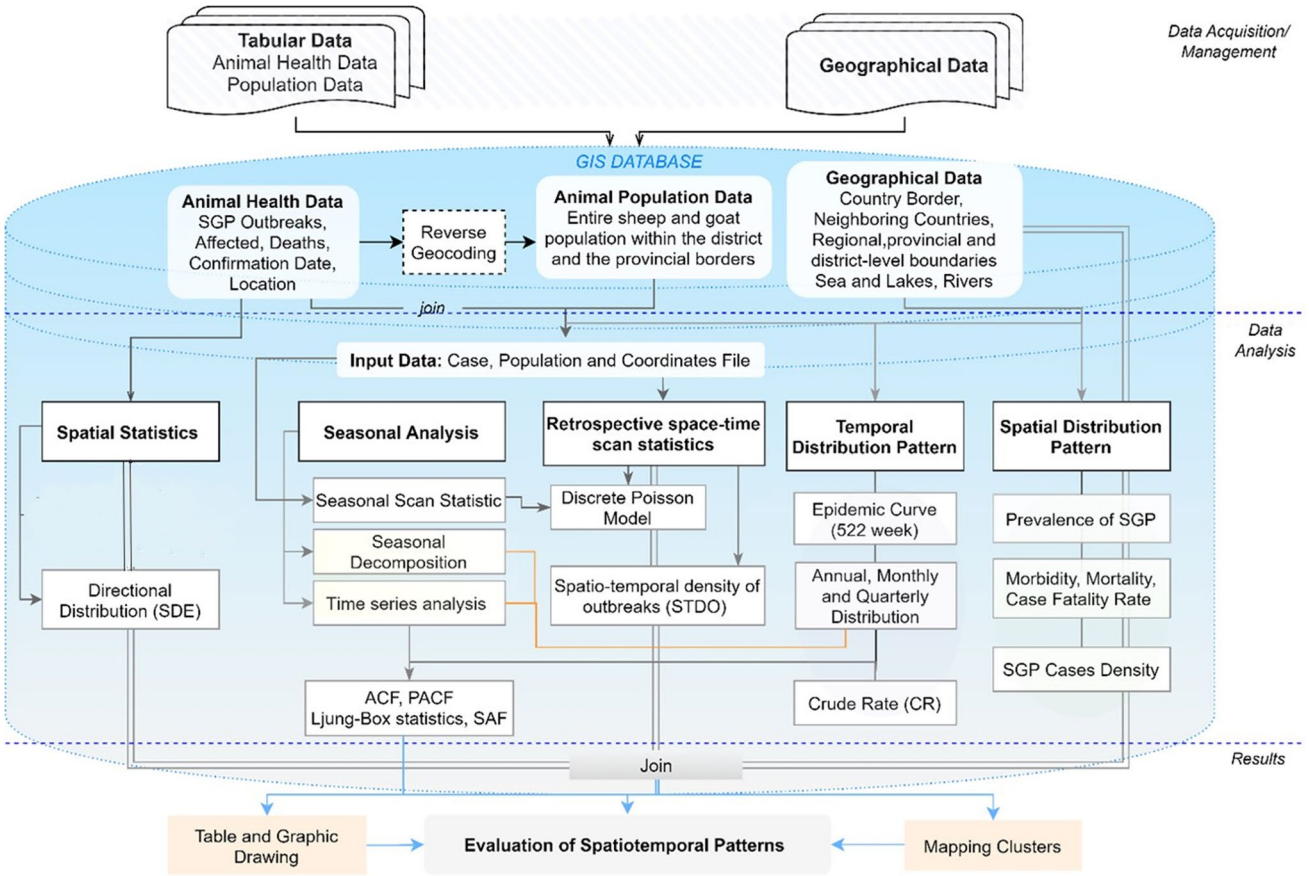

Fig. 2 The workflow followed in the study

Retrospective space–time scan statistical analysis

Kulldorff's space–time scan statistic based on the Poisson model was used to detect significant clusters of SGP cases during the study period. Spatiotemporal and seasonal retrospective scan analyses were applied to analyze and evaluate clusters of the highest SGP incidence at the district level. The method was based on the construction of a space–time dynamic cylindrical window in which the base of the cylinder is the spatial scanning window, and the height reflects the temporal scanning window (Fig. 3) (Kulldorff 1997).

The expected and observed numbers of cases are calculated for each cylinder and performed a maximum likelihood test with the null hypothesis. The number of expected cases μ is calculated by Eq. 2.

$$\mu = p * \frac{C}{P} \tag{2}$$

where p is the sheep and goat population inside the scan window, C is the total number of SGP cases in Turkey, and P is the total estimated population during the study period in Turkey. Each scan window is compared to the null hypothesis of a random Poisson distribution, accounting for the population size. The likelihood ratio (LR) test is used to define the difference in the SGP

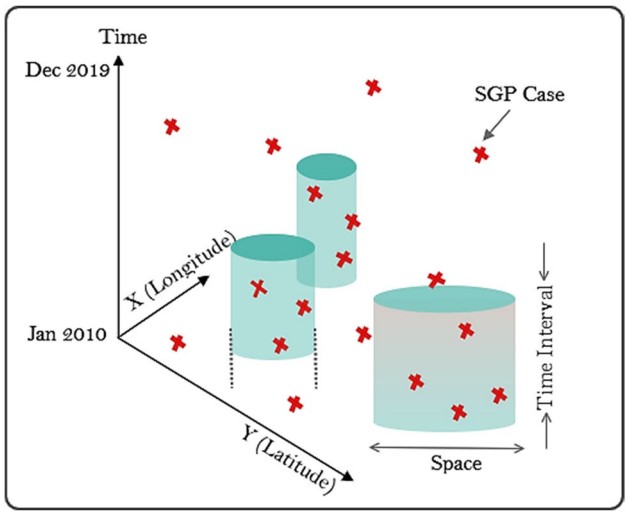

Fig. 3 Space–time scan statistic methodology (adapted from Ahmadkhani et al. 2018)

incidence inside and outside the windows, which is defined in Eq. 3.

$$\frac{L(Z)}{L_0} = \frac{\left(\frac{n_Z}{\mu(Z)}\right)^{n_Z}\left(\frac{N-n_Z}{N-\mu_{(Z)}}\right)^{N-n_Z}}{\left(\frac{N}{\mu(T)}\right)^{N}} \quad (3)$$

where $L(Z)$ is the likelihood function for candidate cylindrical window Z, L_0 is the likelihood function under the null hypothesis, n_Z is the observed number of SGP cases within the cylindrical scan window, $\mu(Z)$ is the expected number of SGP cases within the scan window Z, N is the number of observed cases in the entire districts during study period, and $\mu(T)$ is the total number of expected cases in Turkey during the entire study period. The scan cylinder is reported high risk if the likelihood ratio is greater than 1.

Monte Carlo simulation ($n=999$ permutations) was performed to assess the statistical significance of space–time clusters. The most likely cluster defined the window with the maximum log-likelihood ratio (LLR). Other significant windows are called as the secondary cluster. Clusters were reported if they are statistically significant at p values below 0.05 level and used for further analysis (Ochwo et al. 2018; Li et al. 2019). The maximum radius of the circular base for the possible spatial window size was set to 50% of the total sheep and goat population at risk and the maximum height of the cylinder for temporal window size 50% of the total study period. The unit of the length of time interval of the temporal scan window for a cluster was defined to month because of the low temporal resolution of available data. Furthermore, SGP outbreak locations were indicated as district centroids. The relative risk (RR) was defined to visualize the distribution of risk inside significant clusters and each district belonging to within-cluster (Desjardins et al. 2020). Lastly, for each epidemic district, within-cluster was reported if RR value is greater than 1. RR is defined in Eq. 4.

$$\mathrm{RR} = \frac{c/e}{(C-c)/(C-e)} \quad (4)$$

where c is the total number of observed SGP cases in a district, e is the total number of expected SGP cases in a district, and C is the total number of observed SGP cases in study area. A relative risk is calculated as the estimated risk within a window divided by the risk outside of the window. The possibility of being exposed to SGP of the sheep and goat population within a district was estimated by RR.

Analysis of the spatiotemporal patterns of SGP spread within clusters

The rate of outbreak spread within space–time clusters is roughly estimated using spatiotemporal density of outbreaks (STDO), which determines the number of new outbreaks in a given area over a fixed period of time (Abdrakhmanov et al. 2018; Andrey et al. 2020). The outbreak propagation rate of space–time clusters is calculated with Eq. 3: The calculation was used as described in Eq. 5.

$$\mathrm{STDO}_n = N_n^{obs}/(\pi R_n^2)/T_n * 1000, (\mathrm{km}^{-2}\mathrm{month}^{-1}) \quad (5)$$

where N_n^{obs} is the number of observed outbreaks in the n th cluster; R_n is the radius of the nth cluster, which is used to calculate the area of the circle; and T_n is the duration of the n th cluster in months. The spatiotemporal scale of the STDOs was adjusted to report as the number of outbreaks in 1000 km^2 and 1 month.

Directional distribution analysis

The standard deviational ellipse (SDE) analysis was used to reveal the spatial characteristics and the changes in the directional trend of reported SGP outbreaks for each year in the study area. SDE analysis is often used to determine whether the distribution of a disease shows a directional trend and to visualize the main regions infected (Chen et al. 2020). The spatial distribution ellipse received the coordinates X and Y from the mean center of the spatial distribution of SGP outbreaks as the center and calculated the standard distance separately in the x- and y-directions so that the axes of an ellipse are defined. Then, the method shows the standard deviation from the mean center. Furthermore, this method calculates the major axis, minor axis, and azimuth as base parameters for describing the central tendency, dispersion, and trend direction of the spatial distribution of SGP outbreaks. The direction with the more spatial distribution of SGP outbreaks is represented by the major axis direction of the ellipse and the direction with the less spatial distribution of SGP outbreaks is represented by the minor axis direction. The length of the major axis reflects the degree of deviation of the spatial distribution of elements from the center in the main direction. The azimuth reflected the main trend direction of the distribution, and the ratio of the lengths of the major axes and minor axes reflects the shape of the spatial dispersion tendency (Shan et al. 2021; Abd Majid et al. 2021). The main parameters of SDE are derived by calculating the following:

$$\mathrm{SDE}_x = \sqrt{\frac{\sum_{i=1}^{n}(x_i-\overline{X})^2}{n}} \quad (6)$$

$$\mathrm{SDE}_y = \sqrt{\frac{\sum_{i=1}^{n}(y_i-\overline{Y})^2}{n}}$$

where x_i and y_i denote the latitude and longitude coordinates of SGP outbreak points, respectively, n is equal to the total

number of SGP outbreak points, and $\{\bar{x}, \bar{y}\}$ represents the weighted mean center of the entire SGP points.

$$\tan\theta = \frac{\left(\sum_{i=1}^{n}\tilde{x}_i^2 - \sum_{i=1}^{n}\tilde{y}_i^2\right) + \sqrt{\left(\sum_{i=1}^{n}\tilde{x}_i^2 - \sum_{i=1}^{n}\tilde{y}_i^2\right)^2 + 4\left(\sum_{i=1}^{n}\tilde{x}_i\tilde{y}_i\right)^2}}{2\sum_{i=1}^{n}\tilde{x}_i\tilde{y}_i} \quad (7)$$

$$\sigma_x = \sqrt{2}\sqrt{\frac{\sum_{i=1}^{n}\left(\tilde{x}_i\cos\theta - \tilde{y}_i\sin\theta\right)^2}{n}} \quad (8)$$

$$\sigma_y = \sqrt{2}\sqrt{\frac{\sum_{i=1}^{n}\left(\tilde{x}_i\sin\theta + \tilde{y}_i\cos\theta\right)^2}{n}} \quad (9)$$

where θ denotes the azimuth and indicates the orientation of the ellipse which it represents the rotation of the major axis measured clockwise from noon; $\tilde{x}_i$ and $\tilde{y}_i$ denote the deviation of the *xy*-coordinates from the mean center; and σ_x for the ellipse major axis (long axis) and σ_y for the ellipse minor axis (short axis) represented the standard deviations for the axes *x* and *y* of ellipse which include two standard distances. Finally, the weighted standard deviational ellipse was used, ellipse size was adjusted 1_STANDARD_DEVIATION, and the weight field was represented with the number of SGP cases.

Software tools

The graphics and tables were drawn and visualized with Microsoft Excel 2016 (Microsoft Corp., Redmond, WA, USA). Reverse geocoding at the district level by coordinates of SGP outbreaks was conducted using MMQGIS plugin in QGIS v3.16. The seasonal decomposition of SGP outbreak time series was performed using IBM SPSS Statistics 26.0. The epidemic curve of SGP incidence was drawn by "incidence" package in R v4.0.4 (R Development Core Team). The space–time and seasonal scan statistic was measured with SaTScan 9.6 software. All the maps and documentation processes were obtained using Esri ArcGIS 10.4. The standard deviational ellipse tool in ArcGIS was used to analyze the directional tendency of SGP.

Results

Geographical distribution and descriptive analysis of the SGP disease

SGP outbreaks in Turkey were reported between January 7th, 2010, and December 31st, 2019. A total of 934 SGP outbreaks were reported, with an average of 93 (±58.3 SD) outbreaks per year. Except for before 2013 and 2015 to 2016, the number of SGP outbreaks in other years was higher than 100 (Fig. 4). The highest notification rates of SGP were reported in 2013 (18.7% of total reported outbreaks; 175 outbreaks) followed by 2018 (16.9%; 158 outbreaks). During this 10-year period, a total of 20,309 SGP cases were recorded, with an average of 2131 (±1235.9 SD) cases per year. The highest cases were recorded in 2018 (18.4% of total reported cases; 3730 cases) followed by 2014 (15.8%; 3203 cases). Among the total reported cases, the proportions of sheep and goats were 96% (n = 19,450) and 4% (n = 859), respectively. Additionally, a total of 2169 deaths were attributed to SGP, with an average of 1542 (±1046.8 SD) deaths per year.

The locations of all reported SGPs were identified at the district level and used in further analysis. Accordingly, at least one SGP case was diagnosed in 371 out of 973 districts in Turkey. A descriptive analysis of SGP was presented on a regional basis (n = 7), using average annual number of outbreaks, cases, deaths, and population at risk (Table 1). Population at risk was described to the total number of sheep and goats at the district where a SGP outbreak had occurred. The highest incidences of outbreaks at the district level were observed as 3.1 over all 10 years or 0.3

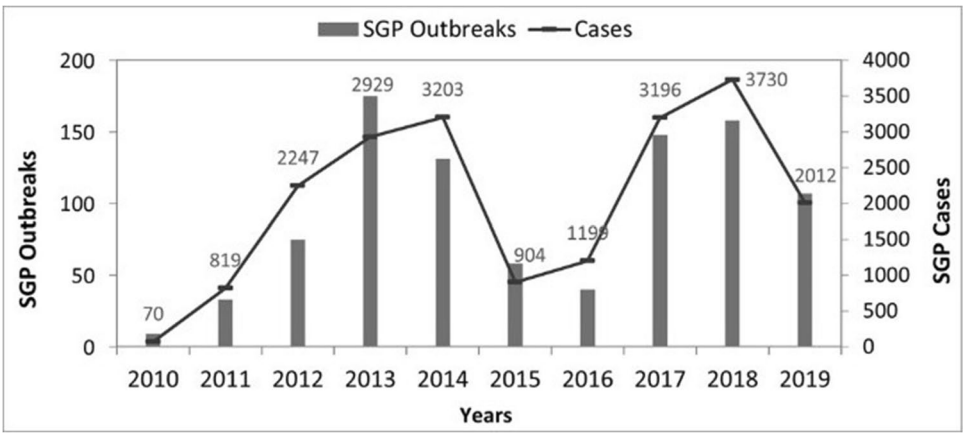

Fig. 4 Total yearly number of sheep and goat pox disease outbreaks and cases in Turkey from 2010 to 2019

per district per year in the Central Anatolia Region (in 97 districts; 304 outbreaks; 31.26% of total reported cases) followed by Marmara Region with 0.3 per district per year (in 72 district; 245 outbreaks; 17.96% of total reported cases). The average incidence in the Aegean Region was 0.23 per district per year (in 60 districts; 137 outbreaks; 12.26% of total reported cases). The Mediterranean Region was 1.6 over all 10 years (in 31 districts; 61 outbreaks; 6.4% of total reported cases) followed by the Black Sea Region with 1.8 per district 10 years (in 60 districts; 109 outbreaks; 12.81%). The lowest incidences were observed in the Southeastern Anatolia Region with 1.4 over all 10 years (in 11 districts; 15 outbreaks; 3.81% of total reported cases) and in the Eastern Anatolia Region with 1.5 (in 41 district; 63 outbreaks; 15.54%). According to the descriptive summary, average annual rates of morbidity and mortality were 103.45 per 100,000 small ruminants and 43.21 per 100,000 small ruminants during this period, respectively. Average annual case fatality rate was 41.76%. In Turkey, it has been determined that SGP outbreak ($n=934$) lasted an average of 41 ($\pm$19.07 SD) days between 2010 and 2019 (Şener 2021).

In order to investigate the density of annual SGP cases by province bases ($n=81$) in Turkey, a SGP case density map was constructed by analyzing the relationship between annual SGP cases and the affected locations which is presented in Fig. 5. The highest density of cases occurred in 2017 and 2018, with 45 and 46 affected provinces, respectively. The highest incidence of SGP outbreaks was reported in Konya province in the Central Anatolia Region all year every year and recorded 58 outbreaks with 716 cases of SGP during this 10-year period.

Incidence of SGP outbreaks adjacent to the international borders

A total of 33 (8.9% of total reported districts) districts close to the international borders of Turkey reported with a total of 73 (7.8% of total reported outbreaks) outbreaks together with 2415 (11.9% of total reported cases) SGP cases. The highest notifications of SGP were reported as 12 outbreaks with a total of 398 cases in 7 districts bordering Iran and 11 outbreaks with a total of 486 cases in 7 districts bordering Syria, followed by 6 outbreaks with 516 cases in 5 district bordering Georgia. A total of 17 outbreaks with 196 cases were reported in 5 districts bordering Greece and Bulgaria between 2013 and 2014, followed by 2017 (70 SGP cases in 1 district). Besides, 6 outbreaks were reported in 5 districts bordering Armenia, with a total of 170 cases.

Directional trend analysis

The directional distribution of the outbreak spread by years as described by the SDE is presented by the visualization results of the standard deviation ellipse analysis in Fig. 5 and the parameter table of the SDE in Table 2. The change tendency of the main orientation was examined by the azimuth of the ellipse's major axis. In 2010, 2013 to 2014, and 2017 to 2018, the deflection angle of the major axis was within the range of 95–124° and the spatial direction of spread of SGP outbreaks displayed NW–SE distribution. Surprisingly, by large scale changes in 2012 to 2013, 2015 to 2016, and 2019, the deflection angle of the major axis showed a decrease within the range of 74–87°, which meant that the major axis is a counterclockwise shift. At the same time, the spatial direction of spread maintained an overall NE–SW distribution. In terms of spatial pattern changes in spread of SGP during the time period, the center of weight moved mainly west by east. Since 2010, the moving of weighted mean center was observed: NE–NW–NW–SE–SW–SE–SW–SE pattern.

The spatial dispersion tendency was analyzed with the ratio of the lengths of the major axes and minor axes. At that, the greater the ratio between the semi-major axis and the semi-minor axis, the more substantial the directionality of SGP outbreaks. The increase of the major axis and lengthening of the minor axis display

Table 1 Average annual number of outbreak, disease, death, and case fatality rates in different regions of Turkey

Region	No. of outbreaks	Population at risk*	No. of cases	No. of dead	Incidence rate (%)	Mortality rate (%)	Case fatality rate (%)
Mediterranean	6	178,676	129	36	0.07	0.02	27.91
Eastern Anatolia	6	423,732	316	131	0.07	0.03	41.46
Aegean	14	220,742	249	72	0.11	0.03	28.92
Southeastern Anatolia	2	202,874	77	34	0.04	0.02	44.16
Central Anatolia	30	582,494	635	308	0.11	0.05	48.50
Black Sea	11	106,446	260	151	0.24	0.14	58.08
Marmara	25	248,223	365	116	0.15	0.05	31.78
Total	93	1,963,186	2031	848	0.10	0.04	41.75

*Population at risk refers to the number of susceptible sheep and goats in the district level for which at least one case has been reported

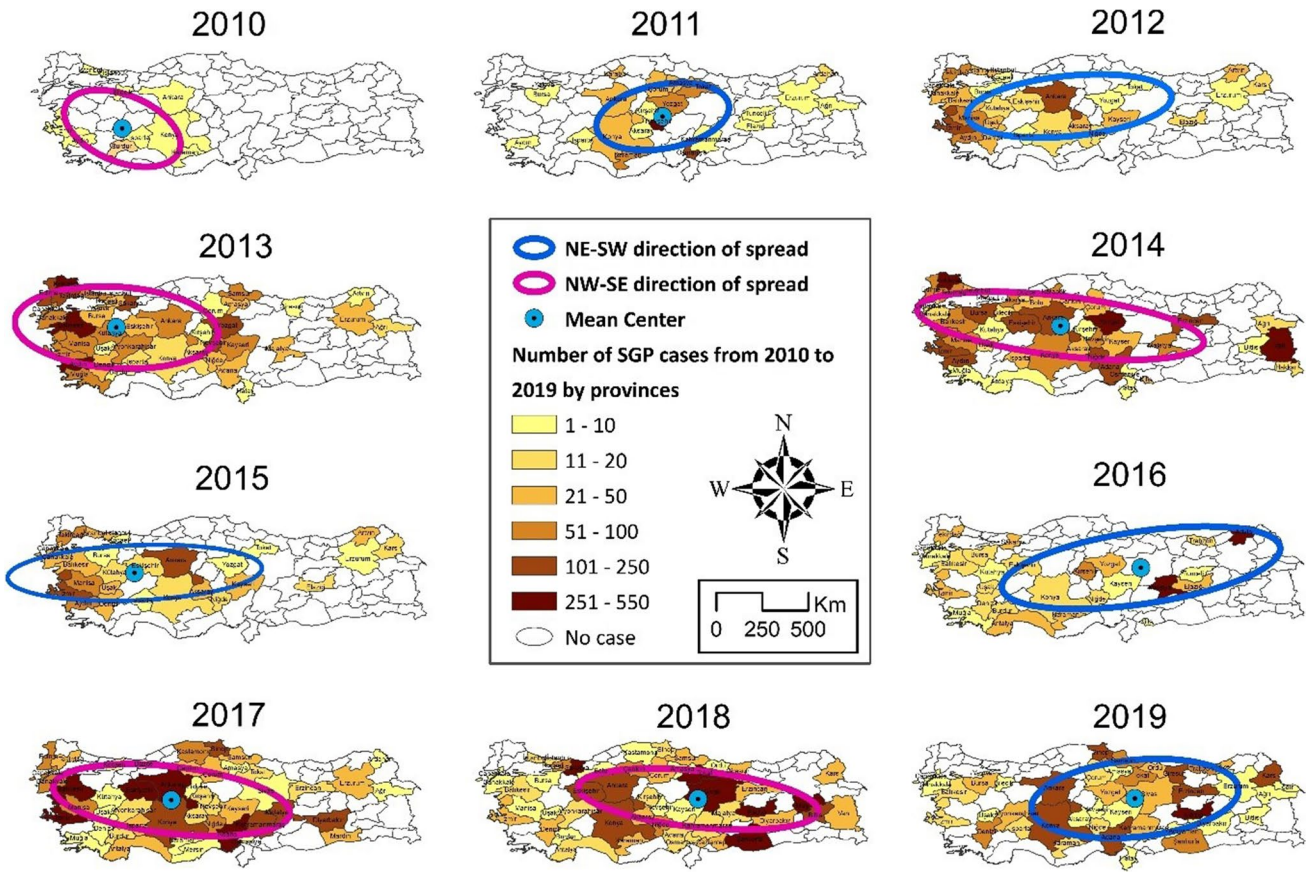

Fig. 5 Directional distribution of SGP cases and annual SGP case density by province between 2010 and 2019

Table 2 The parameter values of the standard deviation ellipses of SGP outbreaks in Turkey from 2010 to 2019

Year	Mean canter (°)		Semi-major axial length (km)	Semi-minor axial length (km)	Long axis/ short axis	Rotation angle (°)
	Longitude	Latitude				
2010	30.11462	38.34804	350.84	221.11	1.59	123.90
2011	34.87948	39.03343	369.79	220.59	1.68	74.01
2012	33.28649	39.37985	591.28	221.99	2.66	82.35
2013	29.93419	39.55179	556.34	285.63	1.95	95.38
2014	32.95209	39.4664	788.85	208.45	3.78	98.94
2015	30.57346	39.25837	693.52	193.93	3.58	86.93
2016	36.86362	39.47609	771.80	252.55	3.06	78.70
2017	32.62605	39.11886	650.97	233.47	2.79	98.89
2018	36.55185	39.20754	658.93	195.92	3.36	97.83
2019	36.54991	39.35339	567.56	268.60	2.11	82.07

that the range of the spread of SGP outbreaks increased in east–west and north–south directions, respectively. The semi-major axial length of weighted SDE increased between 2011 and 2012 by 221 km/year with a ratio from 1.68 to 2.66 and between 2013 and 2014 by 230 km/year with a ratio from 1.95 to 3.78. Since 2012, the semi-major axial length was generally kept above 500 km, and there was a peak in 2014, with a ratio of 3.78. From 2016 to 2019, its general length decreased by 204 km (Table 2). Besides, 2018 and from 2014 to 2016 were higher than other years of spatial contraction between north and south.

Time series description and analysis of SGP data

The highest notification rates of SGP were reported in 2013 (175 outbreaks) which accounted for 18.7% of all outbreaks reported followed by 2018 (158 outbreaks) accounting for 16.9% of all outbreaks reported. Except for before 2013 and 2015 to 2016, the number of SGP outbreaks in other years was higher than 100. Table 3 shows the average monthly incidence of outbreaks over all years, the trend of weekly SGP in Fig. S1. The highest incidence of SGP outbreaks was reported in the month of February (15.0% of total outbreaks reported; 140 outbreaks) followed by January (13.1%; 122 outbreaks across all years). Among the months, June had the lowest incidence of outbreaks which accounted for 4.5% of all outbreaks reported followed by August which accounted for 4.7%. Single factor ANOVA analysis showed significant variation in the incidence of outbreaks between the months ($p = 0.007$); there was a significant difference between February and June ($p = 0.044$).

The components of SGP outbreak time series were estimated by using the additive model of seasonal decomposition over 120 months (over all 10 years). The Ljung–Box (modified Box–Pierce) test was used to provide an estimate of the proportion of the total variation in the series; it detected no outliers in the data (stationary $R^2 = 0.696$; Ljung–Box statistics 8.542; $d.f = 15$; $p = 0.900$). The stationary squared with a value of 0.696 meant that the model could account for 69.6% of the observed to variation in the series. A significant peak ACF at lag 12 was observed by evidence of cyclical fluctuation in the occurrence of outbreak (autocorrelation 0.289; Ljung–Box statistics ($p < 0.001$); a peak PACF at lag of 12 = 0.308). Figure 6A displays number of monthly outbreaks with the seasonality adjusted series and smoothed trend-cycle component (Fig. 6B), seasonal adjustment factor (SAF; Fig. 6C), and irregular components (Fig. 6D). Considering that the peak of seasonally adjusted series exceeded the smoothed trend-cycle series, this showed that the reported rates change with sensitivity to seasonal changes. SGP time series with no seasonal variation have a seasonal component of 0. The peak of seasonal variation was defined by the seasonal adjusted factor (SAF) which is the seasonal component of the decomposed SGP time series for each month, shown in Table 3. The highest SAFs were identified as February (about 7.1) followed by January (about 5.2). Among these months, June (about − 3.8) had the lowest SAF. This indicates that the number of SGP outbreak peaks in October and has a low trough in May. Except for the months of January, February, March, and December were SAF of below 0 (Table 3).

Table 3 Monthly mean numbers and crude rate (CR) of SGP notifications between 2010 and 2019

Months	Mean notification	SAF[a]	Mean cases	CR[b]
January	12.2	5.22	431.8	1.08
February	14	7.10	323.8	0.81
March	9.1	1.51	338.7	0.85
April	8.3	0.86	109.8	0.27
May	5.4	− 2.53	94.8	0.24
June	4.2	− 3.81	112.3	0.28
July	5.3	− 2.51	67	0.17
August	4.4	− 3.38	65.4	0.16
September	5.5	− 2.99	92	0.23
October	7.8	− 0.04	113.7	0.28
November	5.9	− 2.36	73.1	0.18
December	11.3	2.92	208.5	0.52

[a]Seasonal adjustment factor [b]Crude rate unit: cases per 100,000 sheep and goat population

The presence of a seasonally based trend change was analyzed for reported SGP cases by dividing the year into 3-month periods: winter (Q1, December to February), spring (Q2, March to May), summer (Q3, June to August), and fall (Q4, September to November). The peak season of the SAF of registered SGP cases was mainly defined in the winter with SAF of 504.6; that is, in this season, reported SGP cases were more than 504.6% above the other seasons (Table S1). Among these months, the peak of transmission was occurred in January (SAF of 295.4) when the threat is more than 295.4% above the typical months, followed by February and December that have SAFs of 173.5 and 26.1, respectively. The seasonality of transmission was estimated in the spring with SAF of 35.3 (largest in March with of 189.2 SAF); there were the months of April and May with SAF of below 0. Moreover, the lowest transmission was occurred in the seasons of summer and fall, and there were the least SAFs (about − 270), namely, the months of summer and fall have SAF of below 0.

Seasonal scan statistic

The seasonal analysis which ignores the year of the observation and retains only the day and month identified the temporal clusters for the incidence of SGP disease, presented in Table 4. The temporal clusters that were identified from 2010 to 2014 occurred between January 5th and March 2nd. Here, the overall RR within the cluster was 5.2 and that from January 5th to March 2nd was about 5 times more likely to be affected by SGP than in other months. During this peak period, the estimated annual cases within the cluster were 192.5 cases per 100,000 population. The detected temporal cluster in the period 2015–2019 occurred between December 14th and March 30th, and the relative risk had about 4 times higher (RR = 4.26). The estimated annual cases within

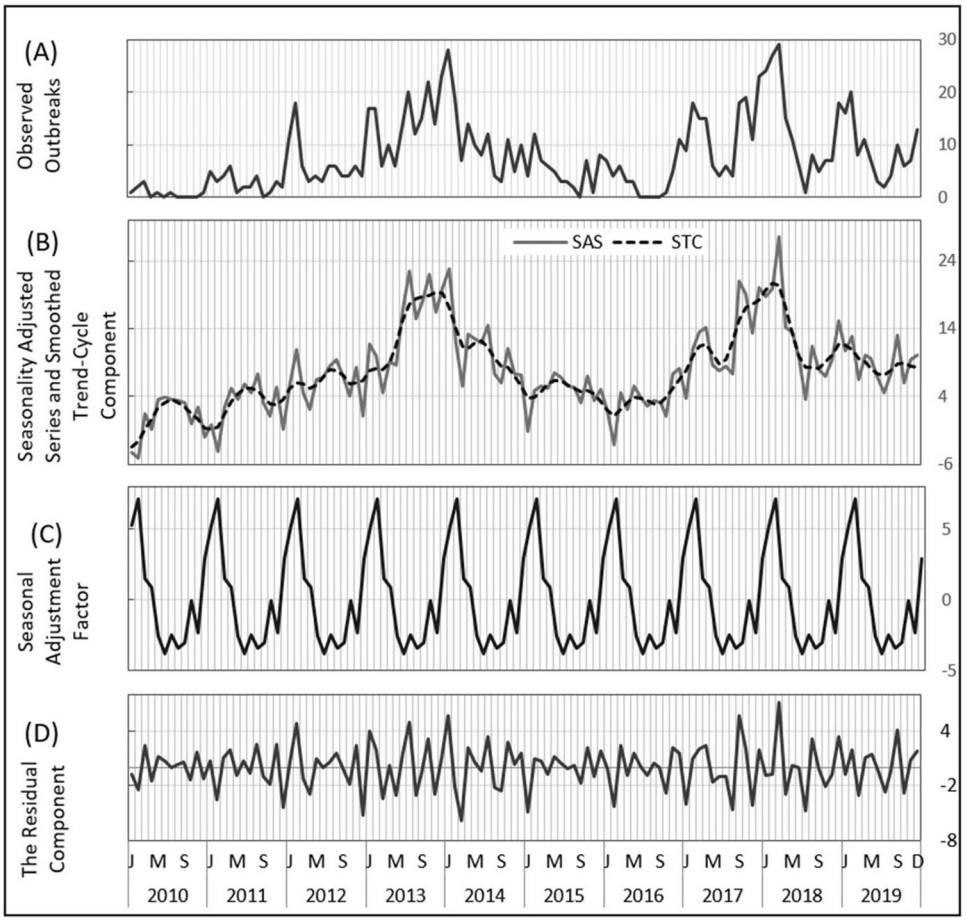

Fig. 6 The seasonal decomposition analysis of SGP outbreaks (each graph has a different *Y*-axis scale). **A**) Observed Outbreaks. **B**) Seasonality Adjusted Series (SAS) and Smoothed Trend-Cycle Component (STC). **C**) Seasonal Adjustment Factor (SAF). **D**) The Residual Component

the cluster were 81.1 per 100,000 during this peak period. The temporal cluster that was identified during the study period (2010 to 2019) occurred between December 14th and March 23rd with annual cases of 97.1 per 100,000. The overall RR within the cluster was 3.84 during the study period. This temporal cluster was around 4 times more likely to be affected by SGP than in other months. The findings of the seasonal clustering support the conclusion of the seasonal decomposition.

Spatiotemporal cluster analysis

Over the study period, spatiotemporal cluster analysis revealed 4 statistically significant clusters of SGP at the district level. The key characteristics of space–time clusters are shown in Table 5 and Fig. 7. The most likely cluster is occurred between January 1st, 2018, and March 31st, 2018, and the center of cluster is in the Kemaliye district in Erzincan province. The radius of the cluster is about 247 km and

Table 4 The temporal clusters of reportable SGP cases in Turkey between 2010 and 2019

Time period	Cluster period	Observed cases	Expected cases	ODE	RR	LLR*	Annual cases per 100,000
2010 to 2014	January 5 to March 2	4466	1405.02	3.18	5.20	2796.64	60.6
2015 to 2019	December 14 to March 30	7163	3340.00	2.14	4.26	2804.63	37.8
2010 to 2019	December 14 to March 23	12,185	5709.81	2.13	3.83	4474.64	45.5

ODE observed divided by expected, *RR* relative risk

*Simulated *p* value, calculated with 999 Monte Carlo replications (*p* value = 0.001)

includes 14 districts with a RR > 1. The overall relative risk (RR) within the cluster was 6.44, indicating that the small ruminant within the region is about 6 times more likely to be exposed to SGP disease than in areas outside the cluster. The 1st secondary cluster was defined between January 1st, 2012, and March 31st, 2012, that its center is located in the Sungurlu district in Corum province, with a RR of about 12 and cluster radius of 99 km and 730 observed cases. This cluster contains 6 districts with a RR > 1. The 2nd secondary cluster was from October 1st, 2017, to December 31st, 2017, that the center of cluster is contained in the Bigadic district in Balikesir province, with 13 districts exhibiting a

Table 5 Spatiotemporal analysis of SGP incidence rates using space–time scan statistic by Poisson model

Cluster	Coordinates/radius (km)	Time frame	Observed cases	Expected cases	RR	Population at risk	LLR[a]	STDO
Adjustment for temporal trend[b]								
Most likely	39.06 N-38.719722 E/246.77	2018/1/1 to 2018/3/31	1814	304.813	6.44	620,713.3	1784.66	0.10
Secondary 1	40.119722 N-34.179722 E/98.95	2012/1/1 to 2012/3/31	730	63.164	11.95	93,448.02	1130.8	0.25
Secondary 2	39.49 N-28.25 E/121.93	2017/10/1 to 2017/12/31	465	65.069	7.29	549,838.6	518.51	0.26
Secondary 3	37.655 N-27.379722 E/40.41	2013/1/1 to 2013/3/31	464	75.295	6.28	5094.75	458.83	0.19

[a]Simulated *p* value, calculated with 999 Monte Carlo replications (p value < 0.001)

[b]Incidence decreased by approximately 9.13% per year

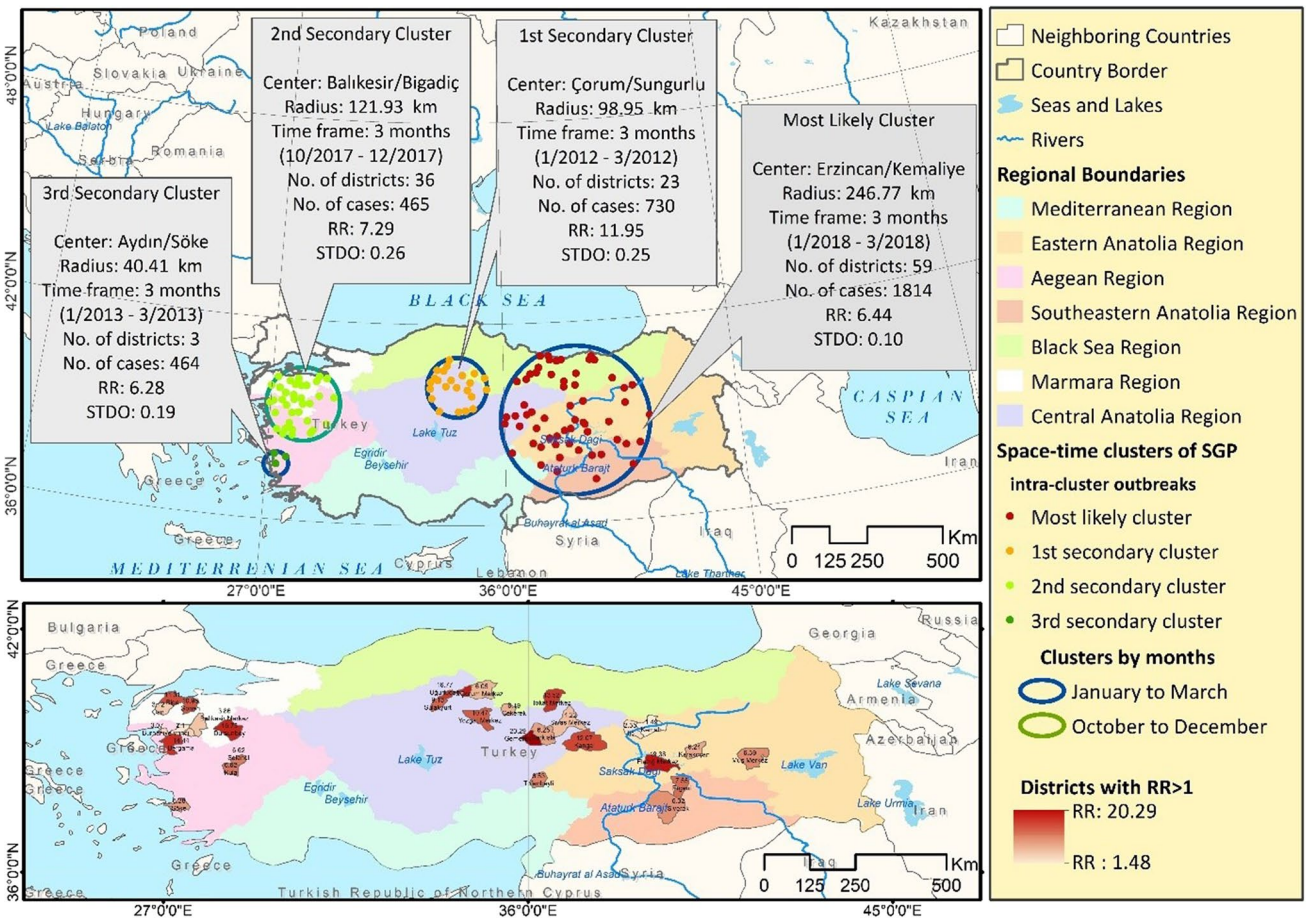

Fig. 7 Space–time distribution of identified clusters of SGP cases with significantly higher incidences in Turkey between 2010 and 2019

RR > 1. The defined overall RR for this cluster was 7.3. The 3rd secondary cluster occurred between January 1st, 2013, and March 31st, 2013, and the center of cluster was located in the Soke district (with a RR > 1) in Aydin province and contains RR of 6.3 within the cluster.

The mean radius of the spatiotemporal clusters was 127.02 km ± 86.90 SD; mean cluster durations (Tn) are 89.75 days ± 0.96 SD, and mean number of outbreaks by observed districts is 30.25 outbreak ± 23.49 SD. Using STDO analysis which represents an indicator of the possible development of an epidemic situation in the case of a new outbreak estimated STDOs of each spatiotemporal cluster. The average STDO was calculated as 0.20 ± 0.07 outbreaks per 1000 km^2 per month.

Supplementary Table S2 illustrates the districts exhibiting a RR > 1 (i.e., more observed than expected cases) in each cluster. The highest relative risk was observed with a RR of 20.3 within the most likely cluster in the Gemerek district in Sivas province, indicating that the population within that district is around 20 times more likely to be affected by SGP. Additively annual SGP incidence rate has been determined to decrease by approximately 9.13% in this study period (Fig. S2).

Discussion

The analysis results evaluating the seasonality for the SGP generally pointed to the wet and cold seasons (December to March). In this study, the seasonality of SGP case reporting peaking in the first quarter (Q1) was also confirmed by time series analysis. The findings showed that the winter season was effective in the contagiousness of the disease for herds and the increase in epidemic reporting peaked in February (Table 3). Although the exact mechanism underlying seasonality is unknown, findings from this study are parallel with the ability of the SGP virus to survive for months in cold and cool environments north of the equator (Hurisa et al. 2018; Yune and Abdela 2017). Finally, findings on SGP seasonality support that vaccination planning in fall season is a correct and effective strategy method to protect herds from the effects of winter season.

Our findings generally agree with the report of studies that the highest number of outbreaks occurred in the winter and spring months, while the lowest outbreaks occurred in the fall and summer months. Similar seasonality in the occurrence of sheep and goat pox has also been reported in other studies in India, Greece, Palestine, Israel, Jordan, and Tunisia (Hailat et al. 1994; Bhanuprakash et al. 2005; Yeruham, et al. 2007; Malesios et al. 2014; Ben Chehida et al. 2018; Atalla and Alzuheir 2019). The differences in SGP seasonality may be due to the difference in the immune status of breeds of sheep and goats in the countries and due to the holding pens of crowded flocks in management (Aregahagn et al. 2021). There may be also various environmental factors that can influence disease occurrence. The peak of SGP outbreaks in cold and wet seasons is emphasized due to the fact that during this period, flocks are exposed to adverse temperatures and in association with the lambing season. Therefore, this might lead them to infection by causing the suppression of their immune system (Malesios et al. 2014).

The spatial variation of the mean center and ellipse orientation over the years in the SDE analysis findings obtained for each year in this study can be explained by the formation of herd immunity within the scope of vaccination for a period of 2 years. Hereof, in the tendency of the main orientation with the azimuth, a pattern that biyearly changes NE–SW or NW–SE tendency was observed (Fig. 5). This situation may indicate the presence of significantly uncontrolled SGP outbreaks in Turkey.

According to the EFSA (2014) report, "up to 40,000 sheep and goats per year are from the provinces affected by SGP in Turkey; It is clearly stated that it was shipped from distant provinces in the east of Turkey, on the border with Armenia, to the provinces in the west of Turkey, including Istanbul, from long distances." The report emphasizes that when SGP cases are detected, restrictions should be imposed immediately, and illegal animal movements, which play an important role in the spread of epidemics in Turkey, should be controlled (Kaymakçı et al. 2000; Cengiz et al. 2015). In a study conducted by the Turkish Agricultural Association (TAA) in 2011, it is stated that around 500 thousand livestock, mostly small cattle, enter Turkey illegally through Iran, Iraq, and Syria every year. It was estimated that the annual economic loss of illegal livestock is around 750 million dollars (Dag and Okde 2016). According to TAA, it was stated that animals stocked around Şanlıurfa and Gaziantep were tried to be transferred from those regions to other regions. Our findings revealed significant endemic hotspots in the east of the country. We guess that the source of infection is likely to originate from the local cluster in the east of the country and that the SGP infection was carried to the west of the country with the animal movements that took place on Eid al-Adha. The reason is that while other space–time clusters are affected by seasonality, the time interval of the 2nd secondary cluster overlaps with the autumn season (Fig. 7). According to the EFSA report, more than 7000 live and ovine animals from 8 different locations were transferred to the cluster area for the 2017 Eid al-Adha. Considering that the 2017 Eid al-Adha coincided with the first week of September, this supports the findings of our study regarding the spread of the disease (Şener 2021).

Local clusters with 6 to 11 times more likely to be exposed to SGP disease than the general distribution

were detected by space–time scan analysis (Table 5). The boundaries of the primary cluster cover an area with a radius of approximately 247 km, framing the Black Sea, Central Anatolia, Eastern Anatolia, and Southeastern Anatolia regions. Districts with RR values within the primary cluster area in Table S2 are priority target response areas for prevention and control of SGP outbreaks. These findings indicate that local differences may be found in the epidemiology of SGP. STDO values can be taken into account by decision makers to compare local outbreak intensities (Table 5).

In general, the winter season is the determining factor for clusters. Here, the time series analysis findings also defined the most intense period of infection as the winter season (Table S1). The results of the space–time clustering analysis support the situation that disease clusters are significantly affected by seasonality and that the disease may have a seasonal process. On the other hand, in the map presented by Thevenin (2011) as "major seasonal movements in Southeastern Anatolia," the most likely clustering area overlaps with the winter quarter (village, camp) areas shown in Elazığ, Diyarbakır, and Şanlıurfa. Elazığ (center) and Diyarbakır (Ergani district) are among the districts with a high relative risk (RR) (Fig. 7). In addition, it was stated in the study that the herds consisted of 400–500 sheep and goats on average, and nomadic transhumance practices were included (Thevenin 2011).

In Turkey, the reporting rates of SGP outbreaks are not known exactly, but there may be limitations due to factors such as transportation and communication, especially in rural areas. This situation can be considered as the reason for the irregular or clinically delayed outbreak reporting. On the other hand, the recurrence of outbreaks may also be based on factors such as the presence of contaminated objects. In this context, effective control studies related to outbreak diameters can be evaluated within the limits of animal movements. Parasitism, bacterial infections, and unregulated trade are considered favorable conditions for the occurrence of SGP disease outbreaks (Aregahagn et al. 2021). The movements of sheep and goats are a major factor facilitating the contact between the infected and susceptible flocks.

The possibility that the SGP outbreaks seen in Greece between 1988 and 2000 and Bulgaria between 1995 and 1996 may have been spread by illegally imported animals from Turkey was emphasized (Mirzaie et al. 2015). Also, hypothetical scenarios of 2013 SGP outbreaks for Greece can be found in the EFSA report (EFSA 2014). The geographical importance of Turkey is taken into account as it may pose a threat to the spread of this disease, which is considered exotic for the EU, over different geographies. At this point, surveillance programs created and effectively used in Turkey are important for the efficiency of export facilities in animal products.

Conclusion

This study, which focuses on the analysis of the distribution of SGP outbreaks reported between 2010 and 2019 in Turkey and includes different statistical methods, has revealed important components in the spatial and temporal dynamics of SGP. Primarily, SGP outbreaks were seasonal and occurred more often during the cold season (winter) which is known to cause stress in animals and compromise the immune system of animals. Generally, spatiotemporal analysis of SGP cases effectively revealed local epidemic occurrence trends and showed that it can be effective in measuring the strength of different disease control strategies. Besides, the calculated STDO values using space–time cluster parameters indicated that they could be utilized as an indicator of the possible spread of an epidemic in the event of a new outbreak. SGP outbreaks were oriented in the northwest-southeast, followed by the northeast-southwest, biennially. Therefore, effective prevention and control measures should be taken to prevent the spread of SGP in the indicated directions. As a result of examining the epidemiology of SGP disease from a spatial perspective, these findings contribute to our understanding of SGP emergence and spread. In conclusion, this study may strategically assist policymakers in disease monitoring and prevention studies and serve as a guide for the routine surveillance and control measures of SGP disease, indicating priority target regions.

Supplementary Information The online version contains supplementary material available at https://doi.org/10.1007/s11250-023-03487-6.

Acknowledgements The authors would like to thank the Ministry of Agriculture and Forestry of the Republic of Turkey for providing the data used in this study.

Author contribution TT put forward the idea. RS carried out the literature research and data analysis. RS and TT fulfilled the data collection, design, interpretation of analyses, and article writing. All authors read and approved the manuscript.

Data availability The data used in this study were obtained from the Ministry of Agriculture and Forestry of the Republic of Turkey. It is not possible to share data without the permission of the relevant institution.

Declarations

Conflict of interest The authors declare no competing interests.

References

Abd Majid, N., Rainis, R., Sahani, M., Mohamed, A. F., Aziz, S. A., & & Nazi, N. M. (2021). Spatial pattern of dengue cases: An analysis in Bangi District, Selangor, Malaysia. Geospatial Health, 16(915), 177 - 182. https://doi.org/10.4081/gh.2021.915

Abdrakhmanov, S. K., Tyulegenov, S. B., Korennoy, F. I., Sultanov, A. A., Sytnik, I. I., & ... & VanderWaal, K. (2018). Spatiotemporal analysis of foot-and-mouth disease outbreaks in

the Republic of Kazakhstan, 1955–2013. Transboundary and emerging diseases, 65(5), 1235–1245. https://doi.org/10.1111/tbed.12864

AHA. (2011). Disease Strategy Sheep pox and goat pox. Animal Health Australia: www.animalhealthaustralia.com.au/programs/emergency-animal-diseasepreparedness/ausvetplan/. Accessed 23 October 2020

Ahmadkhani, M., Alesheikh, A. A., & Khakifirouz, S. &.-V. (2018). Space-time epidemiology of Crimean-Congo hemorrhagic fever (CCHF) in Iran. Ticks and tick-borne diseases, 9(2), 207-216.

Andrey, B., Nadezhda, T., Olga, B., Timofey, S., Andrey, G., Zoran, D., & & Olga, Z. (2020). Spatio-Temporal Analysis of the Spread of ASF in the Russian Federation in 2017-2019. Acta Veterinaria, 70(2), 194-206.

Aregahagn, S., Tadesse, B., Tegegne, B., Worku, Y., & Mohammed, S. (2021). Spatiotemporal Distributions of Sheep and Goat Pox Disease Outbreaks in the Period 2013–2019 in Eastern Amhara Region, Ethiopia. Veterinary Medicine International. https://doi.org/10.1155/2021/6629510

Atalla, H., & Alzuheir, I. (2019). Epidemiological study of sheep and goat pox disease in Palestine during 2005-2017. International Journal of Current Microbiology and Applied Sciences, 8(5), 667-675. https://doi.org/10.20546/ijcmas.2019.805.078

Babiuk, S., Bowden, T. R., Parkyn, G., & Dalman, B. (2009). Yemen and Vietnam capripoxviruses demonstrate a distinct host preference for goats compared with sheep. J. Gen. Virol., 90, 105–114.

Ben Chehida, F., Ayari-Fakhfakh, E., Caufour, P., Amdouni, J., Nasr, J., Messaoudi, L., & ... & Cetre-Sossah, C. (2018). Sheep pox in Tunisia: Current status and perspectives. Transboundary and emerging diseases, 65(1), 50–63.

Bhanuprakash, V., Moorthy, A. R., Krishnappa, G., Srinivasa, R. G., & Indrani, B. K. (2005). An epidemiological study of sheep pox infection in Karnataka State, India. Revue scientifique et technique (International Office of Epizootics), 24(3), 909-920.

Bhanuprakash, V., Hosamani, M., Venkatesan, G., Balamurugan, V., Yogisharadhya, R., & Singh, R. K. (2012). Animal poxvirus vaccines: a comprehensive review. Expert review of vaccines, 11(11), 1355–1374.

Caprarelli, G., & Fletcher, S. (2014). A brief review of spatial analysis concepts and tools used for mapping, containment and risk modelling of infectious diseases and other illnesses. Parasitology, 141(5), 581-601.

Carn, W. M. (1993). Control of capripoxvirus infections. Vaccine, 11, 1275-1279.

Cengiz, F., S., K., Kor, A., Ertuğrul, M., Arık, İ. Z., & Gökdal, Ö. (2015). Küçükbaş hayvan yetiştiriciliğinde değişimler ve yeni arayışlar. Türkiye Ziraat Mühendisliği VIII. Teknik Kongresi Bildiriler Kitabı-2, (s. 809–837). Ankara.

Chen, J., Wang, J., Wang, M., Liang, R., Lu, Y., Zhang, Q., & ... & Niu, B. (2020). Retrospect and risk analysis of foot-and-mouth disease in china based on integrated surveillance and spatial analysis tools. Frontiers in veterinary science, 6(511). https://doi.org/10.3389/fvets.2019.00511

Cromley, E. K., & McLafferty, S. L. (2011). GIS and public health. Guilford Press. New York.

Dag, M., & Okde, B. (2016). The negative factors affecting the border trade in Eastern and Southeastern Anatolia and economic impacts. PressAcademia Procedia, 2(1), 524-534.

Davies, F. G. (1981). Sheep and Goat pox. Virus diseases of food Animals (s. 733–748). London: Academic Press.

Desjardins, M. R., Hohl, A., & Delmelle, E. M. (2020). Rapid surveillance of COVID-19 in the United States using a prospective space-time scan statistic: Detecting and evaluating emerging clusters. Applied geography, 118, 102202.

Dogru, A. O., David, R. M., Ulugtekin, N., Goksel, C., Seker, D. Z., & Sözen, S. (2017). GIS based spatial pattern analysis: Children with Hepatitis A in Turkey. Environmental research, 156, 349-357. https://doi.org/10.1016/j.envres.2017.04.001.

EFSA, P. o. (2014). Scientific opinion on sheep and goat pox. EFSA Journal, 12(11), 3885.

Elliott, P., Wakefield, J. C., Best, N. G., & Briggs, D. J. (2001). Spatial epidemiology: methods and applications. Spatial Epidemiology. Elliott, P., Wakefield, J. C., Best, N. G., & Briggs, D. J. (2001). Spatial epidemiology: m Spatial Epidemiology, 3–14. https://doi.org/10.1093/acprof:oso/9780198515326.003.00

Garner, M. G., Sawarkar, S. D., Brett, E. K., Edwards, J. R., Kulkarni, V. B., Boyle, D. B., & Singh, S. N. (2000). The extent and impact of sheep pox and goat pox in the state of Maharashtra, India. Tropical animal health and production, 32(4), 205-223.

Hailat, N., Al-Rawashdeh, O., Lafi, S., & Al-Bateineh, Z. (1994). An outbreak of sheep pox associated with unusual winter conditions in Jordan. Tropical Animal Health and Production, 26(2), 79-80. https://doi.org/10.1007/BF02239903

House, J. A. (1992). Sheep and goat pox. In: Veterinary Diagnostic Virology: Practitioners Guide. Mosby Year Book.

Hurisa, T. T., Jing, Z., Jia, H., Chen, G., & He, X. B. (2018). A Review on Sheeppox and Goatpox: Insight of Epidemiology, Diagnosis, Treatment and Control Measures in Ethiopia. J Infect Dis Epidemiol, 4, 057.

Kardjadj, M. (2017). Prevalence, distribution, and risk factor for sheep pox and goat pox (SPGP) in Algeria. Tropical animal health and production, 49(3), 649-652.

Kaymakçı, M., Eliçin, A., Tuncel, E., Pekel, E., Karaca, O., Işın, F., & ... & Sönmez, R. (2000). Small sheep and goats breeding in Turkey. V. Technical Congress of Agricultural Engineering of Turkey. 2, 765–793.

Khaliq, A., Batool, S. A., & Chaudhry, M. N. (2015). Seasonality and trend analysis of tuberculosis in Lahore, Pakistan from 2006 to 2013. Journal of epidemiology and global health, 5(4), 397-403. https://doi.org/10.1016/j.jegh.2015.07.007

Kirby, R. S., Delmelle, E., & Eberth, J. M. (2017). Advances in spatial epidemiology and geographic information systems. Annals of epidemiology, 27(1), 1-9.

Kitching, R. P., & Taylor, W. P. (1985). Clinical and antigenic relationship between isolates of Sheep and goat pox viruses. Tropical Animal Health and Production., 17, 64-74.

Kitching, R. P. (2004). Sheeppox and goatpox. In: Coetzer JAW, Infectious Diseases of Livestock. (2nd edn). Southern Africa, Capetown, South Africa: Oxford University Press.

Kulldorff, M. (1997). A spatial scan statistic. Communications in Statistics-Theory and methods, 26(6), 1481-1496.

Kulldorff, M. (2018). SaTScan™ v9. 6: Software for the spatial and space-time scan statistics. Boston, MA, USA.: Department of Population Medicine, Harvard Medical School and Harvard Pilgrim Health Care Institute.

Lee, H. S., Nguyen-Viet, H., Nam, V. S., Lee, M., Won, S., Duc, P. P., & Grace, D. (2017). Seasonal patterns of dengue fever and associated climate factors in 4 provinces in Vietnam from 1994 to 2013. BMC infectious diseases, 17(1), 218.

Li, M., Shi, X., Li, X., Ma, W., & He, J. &. (2019). Sensitivity of disease cluster detection to spatial scales: an analysis with the spatial scan statistic method. International Journal of Geographical Information Science, 33(11), 2125-2152.

MAF. (2018). Combating Animal Diseases and Animal Movements Control Program. Republic of Turkey Ministry of Agriculture and Forestry. https://www.tarimorman.gov.tr/GKGM/Duyuru/326/2018-02-Sayili-Hayvan%C2%A0hastaliklari%C2%A0ile%C2%A0mucadele%C2%A0ve%C2%A0hayvan%C2%A0hareketleri%C2%A0kontrolu-Genelgesi-Yayinlanmistir. Accessed 1 December 2020.

Malesios, C., Demiris, N., Abas, Z., Dadousis, K., & Koutroumanidis, T. (2014). Modeling sheep pox disease from the 1994–1998 epidemic

in Evros prefecture, Greece. Spatial and Spatio-temporal Epidemiology, 11, 1-10.
Mao, Y., He, R., Zhu, B., Liu, J., & Zhang, N. (2020). Notifiable Respiratory Infectious Diseases in China: A Spatial–Temporal Epidemiology Analysis. International journal of environmental research and public health, 17(7). https://doi.org/10.3390/ijerph17072301
Mirzaie, K., Barani, S. M., & Bokaie, S. (2015). A review of sheep pox and goat pox: perspective of their control and eradication in Iran. Journal of Advanced Veterinary and Animal Research, 2(4), 373-381.
Ochwo, S., VanderWaal, K., Munsey, A., Ndekezi, C., Mwebe, R., Okurut, A. R., & ... & Mwiine, F. N. (2018). Spatial and temporal distribution of lumpy skin disease outbreaks in Uganda (2002–2016). BMC veterinary research, 14(1):174, 1–12.
OEI. (2018). Sheep pox and goat pox. OEI Terrastrial Manuel: https://www.oie.int/fileadmin/Home/eng/Health_standards/tahm/3.07.12_S_POX_G_POX.pdf. Accessed 2 December 2020.
Radostits, O. M., Gay, C. C., Hinchcliff, K. W., & Constable, P. D. (2006). Veterinary Medicine E-Book: A textbook of the diseases of cattle, horses, sheep, pigs and goats. Elsevier Health Sciences. (10. b.). SAUNDERS: Elsevier Health Sciences.
Rao, T., & Bandyopadhyay, S. K. (2000). A comprehensive review of goat pox and sheep pox and their diagnosis. Animal health research reviews, 1, 127-136.
Şener, R. (2021). Master of Science Thesis, Department of Geomatics Engineering(145 pp). Turkey: Sivas Cumhuriyet University. Spatial and temporal analysis of sheep pox and goat pox cases by geographical information systems. Turkey.
Shan, W., Wang, Z., Teng, Y., & Wang, M. (2021). Temporal and Spatial Evolution Analysis of Earthquake Events in California and Nevada Based on Spatial Statistics. ISPRS Int. J. Geo-Inf., 10(465). https://doi.org/10.3390/ijgi10070465
Sui, D. Z. (2004). Tobler's first law of geography: A big idea for a small world?. Annals of the Association of American Geographers, 94(2), 269-277.
Thevenin, M. (2011). Kurdish transhumance: Pastoral practices in south-east Turkey. Pastoralism: Research, Policy and Practice, 1(1), 1–24. https://doi.org/10.1186/2041-7136-1-23
TurkStat (2020). Turkish Statistical Institute Central Distribution System: Livestock Statistics. Turkish Statistical Institute. https://biruni.tuik.gov.tr/medas/?kn=101&locale=tr. Accessed 2 December 2020.
Waller, L. A., & Gotway, C. A. (2004). Applied spatial statistics for public health data (Vol. 368). John Wiley & Sons. Inc., Hoboken, New Jersey.
Yeruham, I., Yadin, H., Van Ham, M., Bumbarov, V., Soham, A., & Perl, S. (2007). Economic and epidemiological aspects of an outbreak of sheeppox in a dairy sheep flock. The Veterinary Record, 160(7), 236-237.
Yune, N., & Abdela, N. (2017). Epidemiology and Economic Importance of Sheep and Goat Pox: A Review on Past and Current Aspects. J Vet Sci Technol, 8, 430. https://doi.org/10.4262/2157-7579.1000430